Materials Chemistry and Physics 147 (2014) 492–495

Contents lists available at ScienceDirect

Materials Chemistry and Physics

journal homepage: www.elsevier.com/locate/matchemphys

The chromium site in doped glassy lithium tetraborate

T.D. Kelly [a], E. Echeverria [b], Sumit Beniwal [b], V.T. Adamiv [c], Ya. V. Burak [c], Axel Enders [c], J.C. Petrosky [a], J.W. McClory [a], P.A. Dowben [b, *]

[a] Department of Engineering Physics, Air Force Institute of Technology, 2950 Hobson Way, Wright Patterson Air Force Base, OH 45433, USA
[b] Department of Physics and Astronomy, 855 North 16th Street, Theodore Jorgensen Hall, University of Nebraska-Lincoln, Lincoln, NE 68588-0299, USA
[c] Institute of Physical Optics, 23 Dragomanov Street, Lviv 79005, Ukraine

HIGHLIGHTS

- Adoption of the Li + site for chromium dopants in lithium tetraborate identified.
- Increased oxygen coordination for glass over the crystalline lithium tetraborate.
- Distortions about the doping chromium characterized.
- Local bond order is preserved in spite of the glassy nature.

GRAPHICAL ABSTRACT

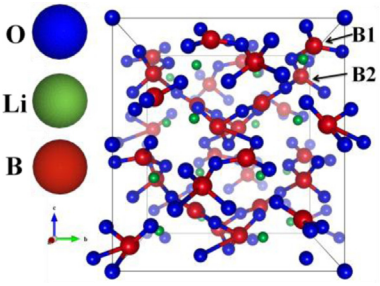

ARTICLE INFO

Article history:
Received 5 February 2014
Received in revised form
9 April 2014
Accepted 10 May 2014
Available online 3 June 2014

Keywords:
Glasses
Oxides
Optical materials
XAFS (EXAFS and XANES)
Microstructure

ABSTRACT

Using extended X-ray absorption fine structure (EXAFS) spectroscopy, we find that Cr substitutes primarily in the Li^+ site as a dopant in lithium tetraborate $Li_2B_4O_7$ glasses, in this case $98.4Li_2B_4O_7{-}1.6Cr_2O_3$ or nominally $Li_{1.98}Cr_{0.025}B_4O_7$. This strong preference for a single site is nonetheless accompanied by site distortions and some site disorder, helping explain the optical properties of chromium doped $Li_2B_4O_7$ glasses. The resulting O coordination shell has a contraction of the Cr–O bond lengths as compared to the Li–O bond lengths. There is also an increase in the O coordination number.

1. Introduction

There has been a huge wealth of studies on Mn doped lithium tetraborate, $Li_2B_4O_7$ [1,2]. Chromium is in many respects very similar, able to adopt a number of nominal valencies from zero valent chromium to chromium +6 (i.e. Cr^0–Cr^{6+}) [3–9]. At first glance, one might think that this means Cr might occupy a wide variety of dopant sites within the $Li_2B_4O_7$ structure. As a dopant, there are very strong indications that Mn can occupy both B and Li sites [1], which is somewhat unusual for $Li_2B_4O_7$ dopants. Electron paramagnetic resonance (EPR) measurements clearly indicate that the chromium dopes $Li_2B_4O_7$ as Cr^{3+} ($3d^3$, $^4A_{2g}$) isolated centers, and further EPR indicates Cr^{3+} isolated centers are at Li^+ sites with strong rhombic distortion and nearly cubic local symmetry consistent with the optical properties [10]. Thus there is every indication that the Cr^{3+} occupies the Li^+ site with residual multi-state character [10].

Occupation of the Li site is important for several reasons. Cr^{3+} centers in high-field sites, where the energy of $^4T_{2g}$ is higher than that of the ^2E_g state, are characterized by narrow emission lines due

* Corresponding author. Tel.: +1 402 472 9838; fax: +1 402 472 6148.
E-mail addresses: pdowben1@unl.edu, pdowben@unl.edu (P. Dowben).

http://dx.doi.org/10.1016/j.matchemphys.2014.05.021
0254-0584/

to the $^2E_g \rightarrow {}^4A_{2g}$ and $^2T_{1g} \rightarrow {}^4A_{2g}$ spin-forbidden transitions. Conversely, the Cr^{3+} centers in low-field sites, where the energy of $^4T_{2g}$ is lower than that of the ^2E_g state, are characterized by broad emission band due to the $^4T_{2g} \rightarrow {}^4A_{2g}$ spin-allowed electron-vibration transition. Both high and low field sites appear to be occupied by Cr^{3+} ions in doped $Li_2B_4O_7$ host [10], and the multisite character of the Cr^{3+} luminescence centers may be the result of disorder in octahedral sites [10]. Additionally, this possible occupation of the Li^+ site is important because along the (001) direction, conductivity appears dominated by Li^+ transport [11–13]. This should lead to some unusual surface segregation effects for dopants occupying the Li^+ site [2], as in the case of Mn doped $Li_2B_4O_7$ where facile temperature dependent Mn surface segregation both to and from the nominally $Li_{1.98}Mn_{0.02}B_4O_7(001)$ is seen to occur [2]. Such surface segregation, with an associated contribution to the ion conductivity in turn could have a profound influence on the net pyroelectric current and stability of the pyroelectric coefficient.

There is an interplay between spin polarization and the Li^+ migration. The migration direction influences the location of the unpaired electron caused by the cation vacancy [12] in lithium tetraborate ($Li_2B_4O_7$); however, the local coordination is also important. Both Cr and Mn have a very large d-moment that may lead to local polarization, as is apparent in Cr and Mn doped boron carbides [14,15], with very different consequences [15]. It is also known that the electronic properties of lithium borates may be manipulated by the direct inclusion of dopants, as well as, by the presence of Li^+, O, and dopant vacancies to serve as trap sites [10,16].

Here, we have investigated the chromium doped glass because a glass is less rigidly fixed to the 104 atoms unit cell of lithium tetraborate ($Li_2B_4O_7$), of the space group I41cd [17–20]. The cell, composed of interlocking BO_3 and BO_4 units, might be somewhat more flexible in the glass, as is indeed observed.

2. Experimental

The chromium doped lithium tetraborate ($Li_2B_4O_7$:Cr) glasses, $98.4Li_2B_4O_7{-}1.6Cr_2O_3$, were fabricated by fast cooling of the melted polycrystalline compounds. Solid-state synthesis of the compound was carried out using a multi-step heating process [10,21]. The Cr impurity was added as Cr_2O_3 at 1.6 mol.%.

The experimental X-ray absorption fine structure (XAFS) was obtained on the double crystal monochromator (DCM) beamline at the Center for Advanced Microstructures and Devices (CAMD) with a DCM of Lemonnier type [22]. Due to the low dopant concentration (nominally 1.6 mol.%), the X-ray absorption spectra were measured in fluorescence mode and the data were not corrected for self-absorption. Multiple scans were made and averaged to improve the signal to noise ratio.

3. Results

The resulting experimental Cr fluorescence signal is plotted in Fig. 1, with the vertical line indicating the K-edge (1s) for Cr at 5989 eV, a value close to the expected Cr K-edge ($E_F - E_K$) [23,24]. Experimentally, the photoelectric origin is estimated from the inflection point of the rising edge to be approximately 6004 eV. Many features appear in the Cr X-ray absorption near edge structure (XANES) region, including the small pre-edge around 5989 eV and a double hump at the top of the white line (sharp rising edge). A similar pre-edge has been observed in Mn doped $Li_2B_4O_7$ crystals [1].

The extended X-ray absorption fine structure (EXAFS) is sensitive to the local physical structure. Consequently, in spite of being a glassy material, with no long range order, the EXAFS is clearly evident, as as may be observed in the absorption oscillations at

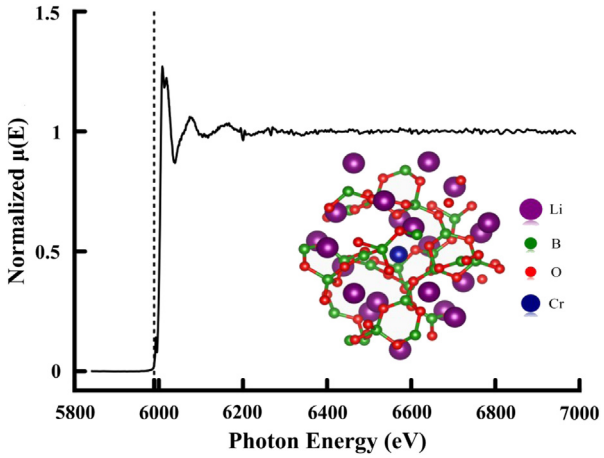

Fig. 1. The normalized experimental X-ray absorption data with a vertical line indicating the Cr K-edge at 5989 eV. The inset illustrates a region of the unit cell with the Cr dopant substituting a Li atom, as used for the FEFF 8 calculations (see text).

energies well above the Cr K-edge. The matrix about the Cr dopant atoms is all a low Z material, and this difficulty is evident in the deterioration of the EXAFS signal into the noise at large wave vector (Fig. 2c). As in the case of other highly defective materials such as the transition metal doped boron carbides [6], also a highly defective material, we can expect that an average bond length and local coordination environment may be extracted from the analysis of the EXAFS data, since the technique does not require long range order.

4. Identification of Cr dopant site

Starting with the unit cell of lithium tetraborate ($Li_2B_4O_7$) [17–20] as the base model is appropriate for ascertaining the preferential Cr dopant site. We may assume that the Cr dopant will either substitutionally dope for the Li^+, occupy a interstitial site, or occupy a B site, but based on prior studies of Mn doping of lithium tetraborate ($Li_2B_4O_7$:Mn) single crystals [1], the Li^+ and B sites must be the most likely. In fact, one preferential site, the Li^+ site indicated in the insert to Fig. 1, seems favored by the chromium dopant, consistent with the conclusion of prior studies [10].

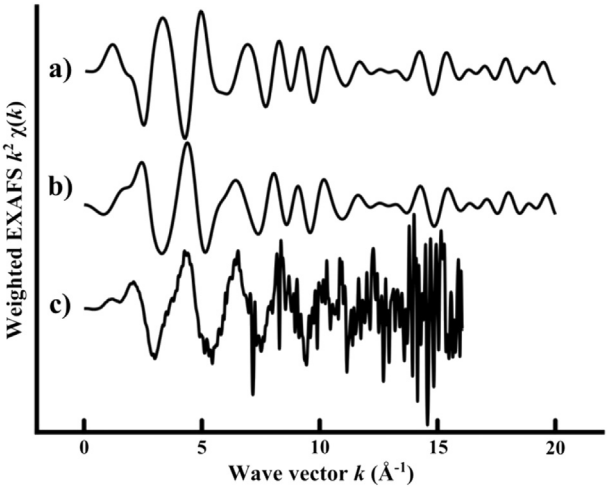

Fig. 2. Model calculations of the k weighted X-ray absorption fine structure, as a function of wave vector of (a) undoped lithium tetraborate (Li absorber), (b) Cr doped lithium tetraborate (substituting Li), compared to the experimental data (c).

The FEFF 8 program package [25] was used to calculate theoretical EXAFS spectra for both undoped $Li_2B_4O_7$ and $Li_2B_4O_7$:Cr. Although it is typically unnecessary when considering only the first coordination shell where single path scattering dominates, multiple scattering of up to 4 path lengths were considered. Self-consistent field calculations were made with a cluster radius of 4.0 Å, which included 33 atoms. A small acceleration factor of 0.05 was used for the calculation of the electronic densities to ensure convergence. Although a low Z system, an exchange correlation factor [26] was applied to the ground state.

In Fig. 2, two theoretical EXAFS spectra are compared to the *k*-weighted experimental data. As unrealistic as this might be from an experimental point of view, using Li as the absorbing center and the Li K-edge, a model spectra is obtained (Fig. 2a). Replacing one Li atom in the unit cell by Cr, the model Cr K-edge EXAFS signal has been plotted in Fig. 2b. It is interesting to note that the two calculations, using Li as the absorbing center (Fig. 2a) and Cr in a Li^+ site as the absorbing center (Fig. 2b) lead to model absorbance spectra, as a function of wave vector, that quickly converge starting at approximately 8 $Å^{-1}$. This is an indication that the nearest coordination shells in the crystalline structure may have distortions in the lattice, but generally the unit cell structure is recovered for a crystalline model. It is the similarity of the model spectra, based on the Li^+ site (schematically illustrated in Fig. 1), with the experimental data (Fig. 2c) that lends strength to the hypothesis that the $Li_2B_4O_7$ unit cell may be used as a base model up to at least the first shell.

Fig. 2 illustrates the similarity between the computational (Fig. 2b) and experimental results (Fig. 2c). Some fundamental conclusions may be drawn. First, the bond lengths of the model are slightly longer than those in the experimental data. Although the two spectra are very similar, the computational model provides features that appear similar but fall at slightly shorter wave vectors than observed in the experimental data (Fig. 2). A shorter wave vector component corresponds to longer bond lengths in the Fourier transformation into R-space, as seen in Fig. 3. Second, the amplitude of the experimental features is greater than in the model calculation, ignoring the noise at higher wave vectors. The increase of the amplitude in the k-space signal is generally an indication of increased coordination number, assuming that the amplitude reduction factor S_0^2 remains relatively unchanged.

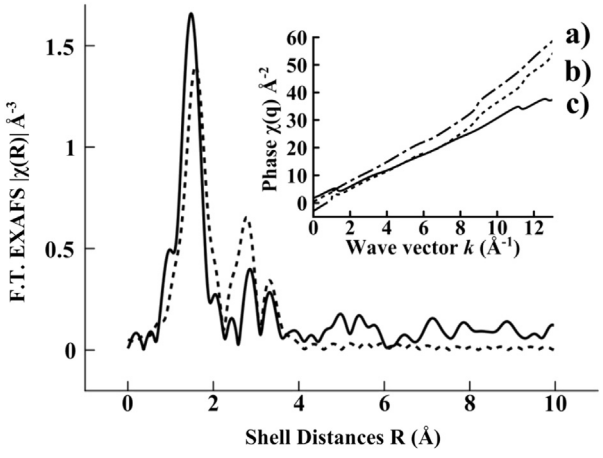

Fig. 3. The Fourier transformed *k* weighted X-ray absorption fine structure (EXAFS). The experimental radial distribution function and phase shifts are plotted as a solid line in both the Figure and the inset respectively. The model radial distribution function and phase shifts (b) about Cr in $Li_2B_4O_7$:Cr are the dashed line in both the figure and the inset. In the inset, the scattering phases for the first shell are plotted for a (a) Li absorber, (b) Cr substituting Li as the absorber, and (c) the experimental data.

We estimated how much the amplitude reduction factor could be expected to vary with a change from a Li absorber to a Cr absorber. In the undoped model calculation (Fig. 2a), the amplitude reduction factor was calculated to be approximately 0.991 while in the Cr doped model the amplitude reduction factor was computed to be 0.955. Thus, it can be safely assumed that since there is little significant change in the amplitude reduction factor S_0^2 that accompanies a replacement of Li with Cr, there must be a change in the O coordination number around the Cr dopant in a Li site. This is in fact consistent with the observed optical properties for $Li_2B_4O_7$:Cr glasses [10]. Considering that the Li^+ ion may have a coordination number between 4 and 5 with an ionic radius between approximately 0.59 and 0.76 Å [27], our model for undoped $Li_2B_4O_7$ having the Li atom surrounded by 4 nearest oxygen atoms at 1.97, 2.03, 2.08, and 2.17 Å (crystalline) seems appropriate. As noted at the outset, the Cr ion may have a variety of charge states [3–10], many of which have an ionic radius comparable with that of the Li^+ ion. Some that may be considered are +2 (high spin, 0.73 Å), +2 (low spin, 0.80 Å), +3 (0.62 Å), +4 (0.55 Å), and +5 (0.57 Å). Almost all of these have a crystalline coordination number of 6, while the +5 state has a coordination number of 8 [3–10,27]. When comparing the theoretical model to the experimental data, it is not unusual to recognize that when the Cr substitutes for Li there is both a slight distortion of the surrounding environment and a decrease in bond length.

As an additional test of the validity of our hypothesis that the Cr dopants substitute in a Li^+ site, the phase shifts have been examined. The EXAFS phase shifts dependent greatly upon the atomic potentials of the (1) species of the scattering coordination shells and the (2) absorbing atoms. These phase shifts are plotted in the inset to Fig. 3. The phase shifts for undoped $Li_2B_4O_7$ and $Li_2B_4O_7$:Cr are plotted as (a) and (b) respectively, while those derived from the experimental data are plotted as (c), in the inset to Fig. 3. The theoretical phase shift from the Cr substituted for Li^+ model is in very close agreement with that of the experimental data (even for $k < 2.0$ $Å^{-1}$). This indicates that the O coordination environment around the Li^+ site, in our model, is closely representative of experiment. At approximately 8 $Å^{-1}$, the phase shift begins to diverge which is an indication that the lithium tetraborate crystal unit cell model breaks down for shells beyond the first shell. This should be expected as the material is a glass and not crystalline.

5. Conclusions

Cr doped lithium tetraborate glasses have been examined using EXAFS spectroscopy. The local order around the Cr dopant is very close to our expectations for the Cr ion substitutionally doping the Li^+ site of lithium tetraborate ($Li_2B_4O_7$). While the Cr ion substitutionally dopes for the Li^+ ion, this doping results in decreased O bond lengths and increased oxygen coordination number. In a glassy material the distortion is easily incorporated due to the relaxed and more randomly oriented nature of the matrix. The conclusions of this study are in agreement with EPR and optical studies which concluded that Cr^{3+} ions substitutionally doping the Li^+ site, but with an increase of O coordination and residual multi-state character [10]. This is important because borates glasses activated by Cr^{3+} ions have the potential for laser generation [10,28].

Acknowledgments

This work was supported by the Nebraska Public Power District through the Nebraska Center for Energy Sciences Research competitive grant program, the Defense Threat Reduction Agency (Grant No. HDTRA1-07-1-0008 and BRBAA08-I-2-0128), the NSF "QSPINS" MRSEC (DMR-0820521) at UNL. The views expressed in

this article are those of the authors and do not reflect the official policy or position of the Air Force, Department of Defense or the U.S. Government.

References

[1] T.D. Kelly, L. Kong, D.A. Buchanan, A.T. Brant, J. Petrosky, J.W. McClory, V.T. Adamiv, Ya. V. Burak, P. Dowben, Phys. Status Solidi B 250 (2013) 1376.
[2] C. Dugan, R.L. Hengehold, S.R. McHale, J.A. Colón Santana, J.W. McClory, V.T. Adamiv, Ya.V. Burak, Ya. B. Losovyj, P.A. Dowben, Appl. Phys. Lett. 102 (2013) 161602.
[3] B.V. Padlyak, A. Gutsze, Appl. Magn. Reson. 14 (1998) 59.
[4] B.V. Padlyak, Cz. Koepke, K. Wislniewski, M. Grinberg, A. Gutsze, P.P. Buchynskii, J. Lumin. 79 (1998) 1.
[5] B.V. Padlyak, A.E. Nosenko, V.M. Maksimenko, V.V. Kravchishin, Phys. Solid State 35 (1993) 1185.
[6] A.E. Nosenko, B.V. Padlyak, Mol. Phys. Rep. 8 (1994) 79.
[7] B.V. Padlyak, J. Kornatowskii, G. Zadrozna, M. Rozwadowski, A. Gutsze, J. Phys. Chem. A 104 (2000) 11837.
[8] N. Ollier, B. Champagnon, B. Boizot, Y. Guyot, G. Panczer, B. Padlyak, J. Non-Cryst. Solids 323 (2003) 200.
[9] B.V. Padlyak, M. Grinberg, T. Łukasiewicz, J. Kisielewski, M. Swirkowicz, J. Alloys Compd. 361 (2003) 6.
[10] B.V. Padlyak, W. Ryba-Romanowski, R. Lisiecki, V.T. Adamiv, Ya.V. Burak, I.M. Teslyuk, Opt. Mater. 34 (2012) 2112.
[11] M. Rizak, V.M. Rizak, N.D. Baisa, V.S. Bilanich, M.V. Boguslavskii, S. Yu. Stefanovich, V.M. Golovei, Crystallogr. Rep. 48 (2003) 676.
[12] M.M. Islam, T. Bredow, P. Heitjans, J. Phys. Condens. Matter 24 (2012) 203201.
[13] A. Senyshyn, H. Boysen, R. Niewa, J. Banys, M. Kinka, Ya. Burak, V. Adamiv, F. Izumi, I. Chumak, H. Fuess, J. Phys. D Appl. Phys. 45 (2012) 175305.
[14] J. Liu, G. Luo, W.-N. Mei, O. Kizilkaya, E.D. Shepherd, J.I. Brand, P.A. Dowben, J. Phys. D Appl. Phys. 43 (2010) 085403.
[15] G. Luo, J. Lu, J. Liu, W.-N. Mei, P.A. Dowben, Mat. Sci. Eng. B 175 (2010) 1.
[16] M.W. Swinney, J.W. McClory, J.C. Petrosky, A.T. Brant, V.T. Adamiv, Ya. V. Burak, P.A. Dowben, L.E. Halliburton, S. Yang, J. Appl. Phys. 107 (2010) 113715.
[17] V.T. Adamiv, Ya. V. Burak, D. Wooten, J. McClory, J. Petrosky, I. Ketsman, J. Xiao, Ya. B. Losovyj, P.A. Dowben, Materials 3 (2010) 4550.
[18] J. Krogh-Moe, Acta Crystallogr. 15 (1962) 190.
[19] J. Krogh-Moe, Acta Crystallogr. B 24 (1968) 179.
[20] A. Witkowska, B. Padlyak, J. Rybicki, J. Non-Cryst. Solids 352 (2006) 4346.
[21] B. Padlyak, W. Ryba-Romanowski, R. Lisiecki, B. Pieprzyk, A. Drzewieki, V. Adamiv, Ya Burak, I. Teslyuk, A. Drzewiecki, Opt. Appl. 42 (2012) 365.
[22] M. Lemonnier, O. Collet, C. Depautex, J.M. Esteva, D. Raoux, Nucl. Instr. Methods A 152 (1978) 109.
[23] J.A. Bearden, A.F. Burr, Rev. Mod. Phys. 39 (1967) 125.
[24] J.H. Hubbell, S.M. Seltzer, Tables of X-ray Mass Attenuation Coefficients and Mass Energy-Absorption Coefficients from 1 keV to 20 MeV for Elements $Z = 1$ to 92 and 48 Additional Substances of Dosimetric Interest, Radiation and Biomolecular Physics Division, NIST, Sep 17, 2009. http://www.nist.gov/pml/data/xraycoef/.
[25] A.L. Ankudinov, B. Ravel, J.J. Rehr, S.D. Conradson, Phys. Rev. B 58 (1998) 7565.
[26] I.N. Yakovkin, P.A. Dowben, Surf. Rev. Lett. 14 (2007) 481.
[27] R.D. Shannon, Acta Crystallogr. A 32 (1976) 751.
[28] J. Mikulski, Cz. Koepke, B. Padlyak, V.T. Adamiv, Ya. V. Burak, Excited State Characteristics of the LBO and KLBO Glasses Activated by Chromium ions, 4th IWASOM Gdansk, Poland, 2013, p. pp.128.